Assessing Net Community Production in a Glaciated Alaska Fjord

Stacey C. Reisdorph[1*] and Jeremy T. Mathis[1, 2]

[1]University of Alaska Fairbanks

Ocean Acidification Research Center

245 O'Neill Bldg.

P.O. Box 757220

Fairbanks, AK 99775-7220

907-474-5995

[2]NOAA - Pacific Marine Environmental Laboratory

7600 Sandpoint Way NE

Seattle, WA 98115

*Correspondence to: S.C. Reisdorph (screisdorph@alaska.edu)

Abstract

The impact of deglaciation in Glacier Bay has been observed to seasonally impact the biogeochemistry of this marine system. The influence from surrounding glaciers, particularly tidewater glaciers, has the potential to greatly impact the efficiency and structure of the marine food web within Glacier Bay. To assess the magnitude, spatial and temporal variability of net community production in a glaciated fjord, we measured dissolved inorganic carbon inorganic macronutrients, dissolved oxygen and particulate

organic carbon between July 2011 and July 2012 in Glacier Bay, AK. Seasonally averaged data were analyzed on a regional basis to account for distinct biogeochemical differences within the bay due to spatial variation in rates of primary production and the influence of glacial-fed stratification, particularly in the northern regions. High net community production rates were observed across the bay (~54 to ~81 mmoles C m^{-2} d^{-1}) between the summer and fall of 2011. However, between the fall and winter, as well as between the winter and spring of 2012, air-sea fluxes of carbon dioxide and organic matter respiration made net community production rates negative across most of the bay as inorganic carbon and macronutrient concentrations returned to pre-bloom levels. The highest carbon production occurred within the lower bay between the summer and fall of 2011 with ~1.3×10^{10} g C $season^{-1}$. Bay-wide, there was carbon production of ~2.6×10^{10} g C $season^{-1}$ between the summer and fall. Respiration and air-sea gas exchange were the dominated drivers of carbon biogeochemistry between the fall and winter of 2012. The substantial spatial and temporal variability in our net community production estimates largely reflect glacial influences within the bay, as melt-water is depleted in macronutrients relative to marine waters entering from the Gulf of Alaska in the middle and lower parts of the bay. Further glacial retreat will likely lead to additional modifications in the carbon biogeochemistry of Glacier Bay with unknown consequences for the local marine food web, which includes many species of marine mammals.

1.0 Introduction

Glacier Bay (GLBA) lies within the Gulf of Alaska (GOA) coastal ocean and is a pristine glacially influenced fjord that is representative of many other estuarine systems that border the GOA (Figure 1). GLBA is influenced by freshwater input, primarily from many surrounding alpine and tidewater glaciers. The low-nutrient influx of freshwater into GLBA, which is highest (up to ~40% freshwater in surface waters during the summer; Reisdorph and Mathis, 2014) along the northern regions of the bay, affects the nutrient loading and, thus, biological production and carbon dioxide (CO_2) fluxes within the bay. The southern region of the bay is less affected by this runoff due to distance from the glacial influence and is more influenced by marine waters that exchange through a narrow channel with a shallow entrance sill.

Alaska's coasts contain more than 200 major fjords, though very few have been studied in detail (Etherington et al., 2007). They can be grouped into two distinct regions, a south-central region and a southeast region, each with hydrological differences due to differences in terrestrial and oceanic influences. The south-central fjords, which include Cook Inlet and Prince William Sound (PWS) (Fig. 1), tend to have more open interaction with the oceanic waters of the GOA, while fjords in the southeast, such as GLBA, communication with the GOA via smaller interconnected channels (Etherington et al., 2007). Glacial influences play an important role in both of these fjord systems, but are more dominant in locations such as GLBA where estuarine-ocean exchange is limited. While PWS and GLBA are highly glacially-influenced and have similar source waters derived from the coastal GOA, PWS is a semi-enclosed fjord that has a relatively direct exchange of waters via Hinchinbrook Entrance and Montague Strait (Musgrave, 2013).

Conversely, GLBA has only one entrance over a shallow entrance sill (~25 m) (Hooge & Hooge, 2002) and connects to the GOA through several small channels (Hill et. al., 2009).

Despite GLBA's limited exchange with the open ocean, elevated chlorophyll-*a* (chl. *a*) concentrations have been observed throughout most of the year, especially from spring through fall (Etherington et. al., 2007) and primary production supports a diverse food web, including endangered species such as humpback whales and Stellar sea lions. Over the past ~250 years, GLBA has experienced very rapid deglaciation, which has likely impacted the biological structure of the bay. As the climate continues to warm, additional changes to this ecosystem and marine population have the potential to impact net community production (NCP) within the bay, with cascading effects through the food web, as has been noted in the GOA in regards to decreasing capelin populations (Arimitsu et al., 2008). To better understand the seasonal dynamics of the underlying biogeochemistry in GLBA, we used the seasonal drawdown of the inorganic constituents of photosynthesis within the mixed layer to estimate regional mass flux of carbon and rates of NCP along with air-sea flux rates of CO_2. This approach has been used in other high-latitude regions to assess ecosystem functionality (e.g. Mathis et al., 2009; Cross et al, 2012; Mathis and Questel, 2013), including net community production and carbon cycling.

Previous studies have shown there is wide-ranging variability in rates of primary production within glaciated fjord systems, though NCP data within these ecosystems are sparse. A study by Whitney (2011) looked at nutrient availability and new production in the subarctic Pacific Ocean between 1987 and 2010. He estimated new production

between April and September of ~7.4 mmoles C m^{-2} d^{-1} off of the Canadian coast (48°-54°N, 140°-128°W) and ~5.5 mmoles C m^{-2} d^{-1} along the subarctic-subtropical boundary in the north-central Pacific Ocean (36°-41°N, 170°-150°W). A comprehensive analysis done by Lockwood et al. (2012) combined previous NCP estimates within the Pacific and GOA regions using a ratio of dissolved oxygen to argon for their NCP calculations. Averaging NCP calculations from their study, as well as multiple publications, they estimated daily NCP around Ocean Station Papa (~50°N - 55°N, 145°W) of 14 ± 5 mmoles C m^{-2} d^{-1}. Additional NCP estimates were done for the northern Pacific region near a chlorophyll front (40°N-45°N) where rates were 9 ± 5 mmoles C m^{-2} d^{-1} and within the Alaska Gyre (~50°N-55°N) where rates were 18 mmoles C m^{-2} d^{-1} (Lockwood et al., 2012).

Fjords within the Central Patagonia region (48°S – 51°S) are strongly influenced by glaciated terrain and freshwater runoff, similar to influences in and around GLBA. A study by Aracena et al. (2011) looked at water column productivity in response to surface sediment export production in various Chilean Patagonia fjords (41-56°S). They divided the fjords into four latitudinal regions and calculated primary production rates during the summer between ~35 mmoles C m^{-2} d^{-1} in the more southern regions (52°S - 55°S) and ~488 C m^{-2} d^{-1} to the north (41°S - ~44°S). In Central Patagonia, Aracena et al. (2011) estimated primary productivity at ~57 mmoles C m^{-2} d^{-1} in the spring, a value comparable to some seasonal estimates in GLBA, and found primary production rates comparable to those of Norwegian fjords (~9 to ~360 mmoles C m^{-2} d^{-1}).

Few regions of the world still have tidewater glaciers, and Alaskan fjords, such as GLBA, is one such region, along with Greenland, Svalbard, Antarctica, Chile, and the

Canadian Arctic (Etherington et al., 2007; Syvitski et al., 1987). Therefore, understanding the dynamics that drive NCP and the associated air-sea CO_2 fluxes within glacially influenced Alaskan fjords can provide insights on how deglaciation may affect carbon budgets and production estimates in fjords worldwide.

There have been a number of studies conducted within GLBA, though conclusions of several studies are contradictory. Many of these studies had a short duration and limited coverage, missing much of the spatial, seasonal, and annual variability (Hooge et al, 2003). To capture some of this seasonal and spatial variability, we collected and analyzed monthly sampling data over a two-year period. This sampling regime, along with the variety of samples taken, has provided us with the most robust data set collected in GLBA and allowed us to elucidate the dynamic nature of NCP in a glaciated fjord.

2.0 Background

Seasonal variation in factors such as light availability, turbulent or wind mixing and freshwater input, impact physical conditions that are vital to primary production, including stratification, photic depth, and nutrient availability. These drivers of NCP vary temporally and spatially within GLBA. Increasing solar radiation during spring and summer help to set up the stratification needed for photosynthetic organisms to remain in the mixed layer and longer daylight hours promote photosynthesis. Low-nutrient glacial runoff is prevalent, and while it aids in stratification, its low macronutrient concentrations dilute available nutrients in the northern regions nearest tidewater outflows. In the lower parts of the bay, glacial influence is lower and macronutrients are more abundant

allowing higher levels of primary production during spring and summer.

GLBA maintains relatively elevated phytoplankton concentrations throughout the year compared to levels observed in similar Alaskan fjords (Hooge & Hooge, 2002). However, insufficient research has been done on the biological system within GLBA to understand why this occurs. One of the more comprehensive studies (Robards et al., 2003) found zooplankton diversity and abundance to be similar to that throughout the GOA. Within GLBA, areas nearest tidewater glaciers, or recently grounded tidewater inlets, maintained some of the highest prey species (i.e. zooplankton and forage fish) abundances, suggesting the importance of these tidewater-influenced habitats. Forage fish, including capelin, sand lance and walleye Pollock, along with euphausids, were generally found the upper inlets and areas near river and stream outlets.

During the summer, GLBA is a crucial locale for several marine predators, some of whose populations are declining due to climate change and deglaciation. Spawning and non-spawning adult capelin, a prey species for several marine predators, are more likely to occur in areas nearest tidewater glaciers that have lower temperatures and chl. *a* levels coupled with higher turbidity and dissolved oxygen concentrations as compared to other areas of GLBA (Arimitsu et al., 2008). In the GOA, populations of capelin, as well as other favored prey species, have been observed to be declining in association with a reduction of these glacially-influenced habitats and have been linked to reduced populations of higher trophic level predators including harbor seals and red-legged kittiwakes (Arimitsu et al, 2008; Piatt and Anderson, 1996; Trites and Donnelly, 2003).

Macronutrient concentrations also vary spatially across the bay, partially due to dilution from the low-nutrient glacial influence in the north. These nutrient

concentrations are also affected by the metabolic requirements of phytoplankton taken up at average proportions for carbon, nitrogen and phosphate of 106:16:1 (e.g. Weber, 2010), referred to as the Redfield ratio. Macronutrient uptake within the southern regions closely follows the Redfield ratio. However, the northern regions are highly influenced by low-macronutrient glacial runoff, resulting in nutrient uptake that deviates from the Redfield ratios.

Reisdorph et al. (2014) found dissolved inorganic carbon (DIC) and total alkalinity (TA) concentrations to be lowest within the upper arms of the bay, while concentrations increased to the south throughout the year, with the largest gradient occurring during summer. However, they found waters across the bay to be well-mixed throughout the water column during winter due to a higher degree of seasonal wind mixing. A similar pattern was observed in the aragonite saturation states (Ω_{Ar}) within the bay with aragonite undersaturation occurring within the upper arms of the bay during though summer. During the fall, Ω_{Ar} were tightly constrained and all surface waters were undersaturated with respect to aragonite.

Aside from primary production, air-sea carbon dioxide (CO_2) flux also impacts carbon concentrations within surface waters. Evans and Mathis (2013) observed instances of both, atmospheric uptake and outgassing, to occur in almost every month in the coastal regions of the GOA, which are the source waters of GLBA. However, uptake of atmospheric CO_2 dominated during the non-winter months, especially in the spring and fall, which coincided with periods of strong winds and undersaturated pCO_2 levels in the surface waters. When annually-averaged, they report that the coastal ocean and continental margin of the GOA act as a strong sink for atmospheric CO_2 with fluxes of -

2.5 and -4 mmoles CO_2 m^{-2} d^{-1}, but their observations were limited in glacially-influenced waters.

For this paper, we have calculated seasonal NCP and air-sea carbon flux for the four regions within GLBA in order to better understand ecosystem production in a glacially dominated environment, representative of much of the southern coastal AK region. This study has greatly enhanced our understanding of how glacial melt impacts the biogeochemistry of estuaries, like GLBA, which are numerous along the GOA coast in Alaska.

3.0 Methods

Ten oceanographic sampling cruises took place aboard the National Park Service's R/V Fog Lark between July 2011 and July 2012. Water column samples were collected at six depths (2, 10, 30, 50,100 m and near the bottom) at each station throughout the bay (Figure 1) with a maximum depth within the west arm of ~430 m. Sampling depths correspond with those currently being used by the Glacier Bay long-term monitoring program and determined by the USGS in the1990s. Each 'core' station (Figure 1) was sampled during every oceanographic sampling cruise, while all 22 stations were sampled during the months of July and January. "Surface" water refers to water collected from a depth of 2 m. unless otherwise stated. Seasonal data was calculated by averaging each measured parameter at each depth for all cruises during the respective seasons. The summer season consists of June, July and August, fall includes September and October; winter is comprised of February and March cruises, and the spring season includes the months of April and May. Data has been averaged regionally within each of

the four regions of the bay (lower bay = LB; central bay = CB; east arm = EA; west arm = WA) (Fig. 1).

Conductivity-temperature-depth (CTD) data were collected on downcasts with a Seabird 19-plus system. Dissolved oxygen (DO) was sampled and processed first to avoid compromising the samples by atmospheric gas exchange. Samples for DO analysis were drawn into individual 115 ml Biological Oxygen Demand (BOD) flasks and rinsed with 4-5 volumes of sample, treated with 1 mL $MnCl_2$ and 1 mL NaI/NaOH, plugged, and the neck filled with DI water to avoid atmospheric exchange. Dissolved oxygen was sampled and analyzed using the Winkler titrations and the methods of Langdon (2010). Samples were analyzed within 48 hours. Apparent oxygen utilization (AOU) was derived from observed DO concentrations using Ocean Data View calculations in version 4.6.2 (Schlitzer, 2013).

DIC samples were drawn into 250 mL borosilicate bottles. Samples were fixed with a saturated mercuric chloride solution (200 µl), the bottles sealed, and stored until analysis at the Ocean Acidification Research Center (OARC) at the University of Alaska Fairbanks (UAF). High-quality DIC data was attained by using a highly precise (0.02%; 0.4 µmoles kg^{-1}) VINDTA 3C-coulometer system. TA was determined by potentiometric titration with a precision of ~1 µmoles kg^{-1}. DIC and TA samples were calibrated by routine analysis using seawater certified reference materials (CRM) prepared and distributed by Scripps Institute of Oceanography, UCSD (Dr. Andrew Dickson's Laboratory) to ensure accuracy. While glacial flour may supply some carbonate minerals to the marine system, influencing DIC and $CaCO_2$ concentrations, we were not able to quantify the amount of glacial flour deposited in the bay or analyze its composition for

this study.

Macronutrient samples were filtered through 0.8 µm Nuclepore filters using in-line polycarbonate filter holders into 25 ml HDPE bottles and frozen (-20°C) until analysis at UAF. Samples were filtered to remove any particles, such as glacial silt, that had the potential to clog equipment during analysis. Samples were analyzed within several weeks of collection using an Alpkem Rapid Flow Analyzer 300 and following the protocols of Mordy et al. (2010).

Particulate organic carbon (POC) samples were collected from Niskins into brown 1 L Nalgene bottles and stored for filtering within 2 days of collection. A known volume of samples was filtered through muffled and preweighed 13 mm type A/E glass fiber filters using a vacuum pump. Muffling involved using tweezers to wrap filters in aluminum foil and heating them at 450°F for ~6 hours in a muffling furnace in order to remove any residual organic material. Filtered sampled were frozen for transport back to UAF where they were then dried and reweighed. Analyses were completed by OARC at UAF and were run using the methods outlined in Goni et al. (2001).

The partial pressure of CO_2 (pCO_2) was calculated using CO2SYS (version 2.0), a program that employs thermodynamic models of Lewis and Wallace (1995) to calculate marine carbonate system parameters. Seasonally averaged atmospheric pCO_2 values (µatm) were used (388.4, 388.9, 393.4, 393.8 and 391.8 for summer 2011 through summer 2012, respectively). Seasonally atmospheric pCO_2 values were averaged from the monthly averaged Mauna Loa archive found at www.esrl.noaa.gov. Seasonally atmospheric pCO_2 values were averaged from the monthly averaged Mauna Loa archive found at www.esrl.noaa.gov. For seawater pCO_2 calculations in CO2SYS we used K_1 and

K_2 constants from Mehrback et al., 1973 and refit by Dickson and Millero (1987), $KHSO_2$ values from Dickson, the seawater pH scale, and $[B]_T$ value from Uppstrom (1974).

CO_2 fluxes were calculated using seasonally averaged seawater temperature, wind speed, and seawater and atmospheric pCO_2 data using the equation,

$$\text{Flux} = L * (\Delta pCO_2) * k \quad \text{(Eq. 1)}$$

where L is the solubility of CO_2 at a specified seawater temperature in mmoles m^{-3} atm^{-1} and ΔpCO_2 represents the difference between seawater and atmospheric pCO_2 in µatm. k is the steady/short-term wind parameterization in cm hr^{-1} at a specified wind speed and follows the equation,

$$k = 0.0283 * U^3 * (Sc/660)^{(-½)} \quad \text{(Eq. 2)}$$

where U is wind speed in m s^{-1}, *Sc* is Schmidt number, or the kinematic velocity of the water divided by the molecular diffusivity of a gas in water, and was normalized to 660 cm hr^{-1}, equivalent to the *Sc* for CO_2 in 20°C seawater (Wanninkhof and McGillis, 1999). Wind speeds were cubed using the methods of Wanninkhof and McGillis (1999) in an attempt to account for the retardation of gas transfer at low to moderate wind speeds by surfactants and the bubble-enhanced gas transfer that occurs at higher wind speeds.

Seawater temperatures for flux calculations were taken from surface bottle CTD data. Wind speeds were obtained from a Bartlett Cove, AK weather station (Station BLTA2) located in GLBA and maintained by the National Weather Service Alaska Region.

NCP calculations were made using the seasonal drawdown of DIC within the mixed layer (upper 30 m) and were normalized to a salinity of 35. NCP production was

calculated for each season between the summer of 2011 and the summer of 2012 according to the equation (Williams, 1993),

$$NCP = DIC_{spring} - DIC_{summer} \quad \text{(Eq. 3)}$$

$$= \Delta DIC \text{ (moles C per unit volume area)}$$

Since this equation only reflects the effects of DIC, freshwater influences on alkalinity were accounted for by correction of the seasonal changes in TA (Lee, 2001) using the equation,

$$\Delta DIC_{Alk} = 0.5*(\Delta Alk + \Delta NO_3) \quad \text{(Eq. 4)}$$

and subtracting this value from the seasonal change in salinity-normalized DIC (nDIC), thus providing an NCP in which the significant process influencing seasonal changes to DIC concentrations is biological productivity (Bates et al, 2005; Mathis et al., 2009; Cross et al., 2012). Air-sea gas exchange can play a lesser role in NCP variation and these are discussed in Section 4.5. Rough regional area estimates were calculated using average lengths and widths of each of the 4 regions. Regional boundaries were selected based on historical and ongoing research in GLBA. Due to the sampling schedule and the small areal size of each region, NCP estimates were calculated using data from stations within each region and averaged to provide one regional estimate for each season. Carbon concentrations used for NCP calculations were not analyzed to determine allochthonous vs. autochthonous organic matter origin.

Figures 1 through 6 were created using Ocean Data View (ODV) version 4.6.2 (Schlitzer, 2013). Figure 7 was created in Microsoft Excel 2008 version 12.3.6.

4.0 Results

4.1 Spatial and seasonal salinity distributions

Salinity distributions throughout the bay were generally the result of the influence of glacial runoff. Salinity was lowest in the surface waters of the east and west arms during the summer of 2011, with a minimum surface salinity of 22.9 at station 20 at the head of the east arm. During this summer season salinity ranged from 22.9 at station 20 to 32.5 in the bottom waters of station 24 just outside the bay's entrance sill. The vertical salinity gradient was strongest in the upper ~50 m of the water column, having salinities of ~31 at 50 m at all stations. Isohalines were horizontal down to ~50 m starting in the upper arms south through the upper portion of the lower bay. Isohalines became vertical in the lower bay and intersected the surface just north of station 01 near the entrance sill. The highest salinities (~31-32) were found in the lower bay at station 01 above the entrance sill and station 24 outside of the sill. These stations experience turbulent mixing across and outside of the sill mixing the more marine waters throughout the water column.

Salinity was more constrained during the fall, with a full water column range between 25.3 in the surface waters at station 07 and 31.4 at depth (~130 m) at station 13. Similar to the previous summer, isohalines were horizontal with a strong vertical gradient in the upper ~50 m, ranging from ~26 at the head of the east arm to ~30 at 50 m depth. Again the isohalines remained horizontal from the upper arms to the mid-lower bay near station 01 where more turbulent mixing across the entrance sill mixed the water column causing isohalines to become vertical and intersect the surface. Salinities in the lower bay near and outside of the bay were between ~30 and 31, with the higher salinities at depth in Cross Sound.

During the winter salinity had a narrow range 29.6 and 31.6. The highest salinities were observed in the bottom waters at station 24, though salinity was similar at all depth at this station with a range from 31.3 to 31.6. The lowest salinities (~30) were within the top 10 m of station 12 located in the upper east arm. In the east arm a water mass with higher salinity (~31) intruded at depth over the entrance sill into the mid to bottom waters of the lower and central bay and was visible in through station 13.

In the spring, salinity continued to have a narrow range, with bay wide salinities between ~28.9 at the surface of station 12 and 31.7 in the bottom water of station 24. Salinities below a depth of 50 m were relatively homogenous at ~31. Salinities were lowest in the surface waters of both arms, with the strongest salinity gradients in the upper 30 m.

Returning to summer conditions in 2012, a strong salinity gradient was observed in the upper 50 m along the east and west arms. Salinities across the bay ranged from 24.1 in the surface waters of station 12 to 32.2, again within the bottom waters of station 24. The lowest salinities were observed in the surface waters at the head of both arms, with this low salinity signal stretching south through the through the central bay. As observed during the previous summer and fall, isohalines were horizontal from the upper arms through the lower-central bay and becoming vertical just north of station 01 where waters became more well-mixed near the sill. Stations within the lower bay had the highest salinities having salinities between ~31 and 32 at all depths.

4.2 Spatial and seasonal distributions of DIC and nitrate

DIC and nitrate are important inorganic components that are consumed during

photosynthesis at various rates throughout the year in GLBA. Figure 2 shows the seasonal relationship between DIC, nitrate and depth between the summer of 2011 and the summer of 2012 with the red line depicting the C:N Redfield Ratio of 106:16.

DIC concentrations during the summer of 2011 ranged from ~1400 to 2100 μmoles kg^{-1}, with the lowest concentrations in the arms and upper-CB. Below the surface layer, DIC and nitrate concentrations followed the Redfield ratio and were fairly constant throughout the year. The lowest concentrations of DIC and macronutrients were observed within the arms.

Nitrate concentrations throughout the water column during the summer of 2011 ranged from ~2.5 to ~37 μmoles kg^{-1}, with slightly less variability in the surface layer (~2.5 and 24 μmoles kg^{-1}). Surface nitrate concentrations were low, but remained >5 μmoles kg^{-1} at all stations. Nitrate values were consistently the lowest in the two arms and CB. While there was a large drawdown of nitrate, particularly in spring and summer (as much as 20 μmoles kg^{-1} when compared to winter concentrations), surface waters were not depleted at any of the observed stations. Additionally, phosphate concentrations (data not shown here) remained above ~0.5 μmoles kg^{-1}.

In the fall of 2011, DIC and nitrate concentrations increased in the surface waters, ranging from ~1700 μmoles kg^{-1} to 2040 μmoles kg^{-1}, while below the surface DIC concentrations reached ~2075 μmoles kg^{-1}. Water column nitrate concentrations during this time were between ~12 μmoles kg^{-1} and 32 μmoles kg^{-1} with similar concentrations within surface waters (11 μmoles kg^{-1} to 30 μmoles kg^{-1}) and the lowest concentrations observed in the arms.

DIC concentrations were much more constrained during the winter (~1920

μmoles kg^{-1} to 2075 μmoles kg^{-1}) than during previous seasons, with little to no significant difference between surface concentrations and those at depth. Nitrate concentrations were similar to those of fall, ranging from ~12 μmoles kg^{-1} to 33 μmoles kg^{-1}. During winter DIC and nitrate concentrations fell near the Redfield ratio, but deviated slightly from Redfield at the highest nitrate concentrations (Fig. 2).

During the spring of 2012 DIC and nitrate had reduced concentrations in surface waters across the bay. Surface DIC concentrations were between ~1750 μmoles kg^{-1} and 2025 μmoles kg^{-1}, with water column concentrations reaching ~2075 μmoles kg^{-1} (Fig. 2). Water column nitrate concentrations ranged from ~7 μmoles kg^{-1} to ~ 31 μmoles kg^{-1}, with an observed surface water maximum of ~20 μmoles kg^{-1}. During the spring DIC and nitrate correlated closely with the Redfield ratio except for two surface samples located at the northernmost ends of each arm (Fig. 2).

Further drawdown of DIC and nitrate in surface waters was observed during the summer of 2012. However, concentrations did not drop as low as was observed during the previous summer. In 2012 DIC concentrations were between ~1545 to 2066 μmoles kg^{-1}, while the surface waters had a maximum of ~2000 μmoles kg^{-1} and, similar to the previous summer, macronutrients did not reach depletion during the summer of 2012. Nitrate concentrations varied from ~13 to 33 μmoles kg^{-1}, with surface concentrations between ~17 and 31 μmoles kg^{-1}. Surface nitrate concentration continued to deviate from the Redfield ratio during this season. The stations with the lowest DIC and nitrate concentrations were those within the EA and WA, as well as the upper CB. Within the LB surface water concentrations fell closer to the Redfield ratio.

4.3 Rates and Masses of NCP

As mentioned in Section 3.0, DIC concentrations in the upper 30 m of the water column, representing the seasonally averaged MLD, were averaged and normalized to a salinity of 35 in order to estimate rates and masses of NCP between seasons (Figure 3).

The seasonal transition between the summer and fall of 2011 had the largest rates of NCP observed during the year of study. Rates of NCP were positive in all regions of the bay and were highest within the east and west arms of the bay at 70.3 ± 3.5 and 81.3 ± 4.1 mmoles C m^{-2} d^{-1}, respectively. A similar NCP rate of 68.9 ± 3.4 mmoles C m^{-2} d^{-1} was observed within the LB, while the CB had the lowest rate between of 53.6 ± 2.7 mmoles C m^{-2} d^{-1}.

Calculated rates of NCP became negative during the seasonal transitions from fall to winter, as well as from winter to spring. Between the fall and winter, the LB experienced the highest degree of CO_2 flux when compared to biological production with a calculated NCP rate of -14.2 ± 0.7 mmoles C m^{-2} d^{-1} followed closely by the CB at -11.5 ± 0.6 mmoles C m^{-2} d^{-1}. Rates of NCP were negative in the east and west arms (-0.5 ± 0.03 and -1.3 ± 0.1 mmoles C m^{-2} d^{-1}), respectively, but to a less degree than in regions to the south.

Between the winter and spring of 2012, rates of NCP remained negative within the east and west arms of the bay, with rates of -36.4 ± 1.8 mmoles C m^{-2} d^{-1} and -26.6 ± 1.3 mmoles C m^{-2} d^{-1}, respectively, and to a lesser degree in CB with -17.5 ± 0.9 mmoles C m^{-2} d^{-1}. A positive NCP rate was estimated for the LB of 17.6 ± 0.9 mmoles C m^{-2} d^{-1}.

Between the spring and summer of 2012 rates of NCP were positive across the bay. The LB had the highest rate of NCP at 19.4 ± 1.0 mmoles C m^{-2} d^{-1}. CB and the EA

had similar rates of 17.2 ± 0.9 and 15.7 ± 0.8 mmoles C m^{-2} d^{-1}, respectively. The WA displayed a lower rate of NCP at 6.0 ± 0.3 mmoles C m^{-2} d^{-1}.

The total mass (g C $season^{-1}$) of carbon produced from NCP was also estimated for each season and are shown in Figure 4. Production of organic carbon occurred between the summer and fall of 2011, with the largest production signal in the LB and decreasing to the north. The LB had the largest biomass production of $1.3x10^{10} \pm 6.5x10^{8}$ g C $season^{-1}$. The CB also had a large amount of production of $5.9x10^{9} \pm 3.0x10^{8}$ g C $season^{-1}$, followed by the west and east arms with $4.9x10^{9} \pm 2.5x10^{8}$ and $2.0x10^{9} \pm 1.0x10^{9}$ g C $season^{-1}$, respectively. When summed across the bay we found ~$2.6\ x10^{10} \pm 1.3x10^{9}$ g C $season^{-1}$ produced between the summer and fall of 2011.

As with some of the rates of NCP, carbon masses were negative during several seasonal transitions. Between the fall and winter the LB had carbon production of -$1.7x10^{10} \pm 8.5x10^{8}$ g C $season^{-1}$, while the east arm had a lower degree of production at -$9.5x10^{7} \pm 4.8x10^{6}$ g C $season^{-1}$. Carbon masses calculated from NCP in CB and the WA were also negative with -$5.0x10^{8} \pm 2.5x10^{7}$ g C $season^{-1}$ and -$8.6x10^{9} \pm 4.3x10^{8}$ g C $season^{-1}$, respectively.

Between the winter and spring of 2012 masses in the east and west arms were estimated at -$2.2x10^{9} \pm 1.1x10^{8}$ and -$3.3x10^{9} \pm 1.7x10^{8}$ g C $season^{-1}$, respectively while the CB had a calculated value of -$4.1x10^{9} \pm 2.1x10^{8}$ g C $season^{-1}$. The LB had a positive NCP mass of $6.3x10^{9} \pm 3.2x10^{8}$ g C $season^{-1}$. Across the bay, we estimated a total of ~ -$3.3\ x10^{9} \pm 1.7x10^{8}$ g C $season^{-1}$ between the winter and spring of 2012.

Transitioning from the spring to summer the LB once again had the greatest production with $8.0x10^{9} \pm 4.0x10^{8}$ g C $season^{-1}$, followed by production within the CB of

$4.5x10^9 \pm 2.3x10^8$ g C season^{-1}. During this time of the year the east and west arms exhibited the lowest biomass production, with an NCP in the WA of $8.5x10^8 \pm 4.3x10^7$ g C season^{-1} and $9.2x10^7 \pm 4.6x10^6$ g C season^{-1} in the EA. NCP across the entire bay totaled ~$1.3x10^{10} \pm 6.5x10^8$ g C season^{-1}.

4.4 Spatial and seasonal distribution of POC

Particulate organic carbon (POC) concentrations were measured at three depths (surface, 50 m, and bottom) for each station and then averaged regionally. Figure 5 shows the regionally averaged POC concentrations and the color bar represents the apparent oxygen utilization (AOU) for each POC samples.

During the summer of 2011 surface water POC concentrations were between ~12 and ~55 μmoles kg^{-1}. Station 20 at the head of the EA had the highest POC concentration at all sampled depths (~2m, ~50 m and ~160 m). POC concentrations in the surface were ~46 μmoles kg^{-1} and ~ 42 μmoles kg^{-1} at depth, with a local minimum of ~30 μmoles kg^{-1} at 50 m. When regionally averaged, the east and west arms had the highest surface POC concentrations of ~35 and ~33 μmoles kg^{-1}, respectively. The WA also exhibited the highest POC concentrations below the surface with ~33 μmoles kg^{-1} at 50 m and at depth. The arms also exhibited negative AOU of ~ -80 and ~ -64 μmoles kg^{-1} in the west and east arms, respectively. The highest positive AOU of ~105 μmoles kg^{-1} was observed in the bottom waters of the CB. The CB POC concentrations below the surface were similar, at ~9 μmoles kg^{-1}, while the surface waters had a POC concentration of ~28 μmoles kg^{-1}. LB had relatively lower POC concentrations, but were similar at all depth with ~15 μmoles kg^{-1}.

POC concentrations decreased, especially within the surface waters during the

fall. A maximum regional POC concentration of ~13 μmoles kg^{-1} was observed in the surface waters of the WA while surface POC across the other regions were similar, falling between ~8 and ~9 μmoles kg^{-1}. Below the surface layer POC concentrations were low, ranging from ~5 to ~8 μmoles kg^{-1} at both 50 m and at depth. Regionally, all AOU values were positive during the fall of 2011. A maximum regional surface AOU (~82 μmoles kg^{-1}) was estimated for the LB and a minimum (~2 μmoles kg^{-1}) in the surface waters of the CB. The LB was relatively well mixed during fall, with the highest DIC concentrations (~2050 μmoles kg^{-1} at all depths) and lowest oxygen saturation (not shown) of any region during this season.

In the winter of 2012 surface water POC concentrations were not found to exceed 20 μmoles kg^{-1} and AOU across the bay were on the order of ~70 μmoles kg^{-1}. Surface POC concentrations during the winter ranged from ~2 to ~15 μmoles kg^{-1}, while POC concentrations at depth were similar, varying between ~3 and 16 μmoles kg^{-1}. When averaged regionally, the POC maximum in the WA of ~11 μmoles kg^{-1} was observed within the surface waters, while the CB had a subsurface maximum at 50 m of ~5 μmoles kg^{-1}. The EA and LB both had maximum POC concentrations in the bottom waters of ~14 and ~9 μmoles kg^{-1}, respectively. POC minima throughout the bay occurred at ~50 m depth and ranged between ~2 and ~9 μmoles kg^{-1}, except at stations 24 in LB and station 13 within the CB where POC was at a local maximum at this depth.

POC concentration in the surface waters increased during the spring of 2012, primarily within northern regions of the bay. The EA had the greatest increase in surface POC (~62 μmoles kg^{-1}) with concentrations decreasing in the surface water to the south. The WA and CB had similar surface POC concentrations of ~35 μmoles kg^{-1}, and ~30

μmoles kg^{-1}, respectively. The LB had the lowest surface POC concentrations with ~13 μmoles kg^{-1}, while having the highest rate of NCP and AOU (~93 μmoles kg^{-1}). The LB subsurface and deepwater AOU values were positive and POC concentrations, ~9 μmoles kg^{-1} each, were the highest among the regions.

All regions had regionally averaged POC maxima in the surface waters during the summer of 2012. AOU values decreased in surface waters across the bay, while rates of NCP were elevated within these waters. Surface concentrations of POC were highest in the EA (~50 μmoles kg^{-1}). Below the surface layer, POC concentrations decreased, ranging from ~4.5 to ~7 μmoles kg^{-1} at 50 m and ~5 to ~8 μmoles kg^{-1} at depth. The WA and CB regions had surface POC concentrations of ~23 μmoles kg^{-1}. The LB exhibited the lowest surface POC concentration with ~13 μmoles kg^{-1}, while experiencing the highest rate of NCP.

4.5 Relationship between DIC and DO

Figure 6 shows the relationship of DIC and DO within Glacier Bay with the C:O Redfield ratio 106:-170 (Anderson et al., 1994) shown by the red line. During the summer of 2011, DO concentrations ranged from ~190 to ~400 μmoles kg^{-1}. All samples below the surface layer, as well as surface samples within the LB followed the Redfield ratio, with concentrations at depth between ~190 and 280 μmoles kg^{-1}. Surface samples of stations within the arms and CB had high DO concentrations and low DIC. Surface DO was higher than that at depth, ranging between ~230 and 400 μmoles kg^{-1}. However, in the LB DIC concentrations remained elevated (~2030 μmoles kg^{-1}) and DO concentrations were low (~240 μmoles kg^{-1}). During the fall, surface samples within the

arms and CB continued to deviate from Redfield. Surface DO concentrations ranged from ~210 to ~330 μmoles kg^{-1} and corresponded with reduced surface DIC concentrations. At depth, DO concentrations varied between ~200 and 280 μmoles kg^{-1} with C:O ratios close to Redfield.

All samples, at the surface and at depth, followed Redfield closely with surface waters having slightly higher DO and lower DIC concentrations than those at depth during the winter of 2012. Surface water DO concentrations were between 250 and ~280 μmoles kg^{-1}, while deeper waters ranged from ~230 to 255 μmoles kg^{-1}.

In the spring, DIC was drawn down and DO concentrations increased, having a range between ~270 and 410 μmoles kg^{-1}. DO concentrations were amplified while DIC was reduced at stations in the northern-most regions of both arms. These samples deviated the most from Redfield, while the remaining samples adhered to the Redfield ratio. Below the surface layer, DO concentration throughout the bay ranged from ~250 to 280 μmoles kg^{-1}

During the summer of 2012, the surface waters within the two arms and CB continued to diverge from Redfield. DIC concentrations within the more northern regions of the bay (EA, WA, and CB) were increasingly drawn down, while DO concentrations remained elevated. Surface DO concentrations ranged from ~260 to ~410 μmoles kg^{-1}, with lower DO concentrations at depth, varying from 200 - ~270 μmoles kg^{-1}.

4.6 Air-Sea gas flux

Monthly pCO_2 was averaged seasonally and regionally in GLBA to identify the spatial and temporal variability of air-sea CO_2 exchange between the atmosphere and the

surface waters of the bay. Figure 7 shows the air-sea fluxes for the four regions of the bay during each season between the summers of 2011 and 2012, with positive fluxes indicating outgassing of CO_2 and negative fluxes representing uptake of CO_2 from the atmosphere into the surface waters. As with our other calculations, the regions of the bay have been divided based on physical influences and while we address the influences to saturation states of each region, we cannot say much about regional ecosystem functionality due to limitations in the understanding of biological systems across the bay. The two northern regions (the EA and WA) are highly influenced by fresh glacial runoff, while the LB has little freshwater influence, but a much stronger marine influence. The CB tends to be the region where these influences become highly mixed. These influences have the potential to impact the ecosystem function and primary production of each region in a different way (e.g. Capelin are primarily found in glacially-influenced waters rather than the more marine-influenced regions). However, more study needs to be done on biological distributions within the bay for a more thorough analysis of regional and bay-wide ecosystem functionality.

During the summer of 2011 winds were relatively low, at ~1.6 m s^{-1}, with surface waters of the CB and the WA were undersaturated with respect to atmospheric CO_2 with pCO_2 values of ~250 μatms. The CB and the WA had reduced DIC concentrations during this summer season and acted as minor sinks (~ -0.3 ± 0.02 mmoles C m^{-2} d^{-1} each). The LB and EA had much higher seawater pCO_2 values of ~488 μatms and ~463 μatms and acted as sources for atmospheric CO_2 of ~0.2 ± 0.01 mmoles C m^{-2} d^{-1} for each region. In the LB and CB surface water temperatures were relatively high at ~8.1°C and 8.5°C, respectively.

During the fall of 2011, winds increased slightly to ~2.0 m s^{-1} and surface waters in all regions of the bay were oversaturated with respect to the atmospheric CO_2. The LB experienced the highest pCO_2 at ~670 µatms and acted as the largest source for atmospheric CO_2 with a flux of ~1.1 ± 0.06 mmoles C m^{-2} d^{-1}. The CB also had elevated pCO_2 with ~510 µatms leading to outgassing of ~0.5 ± 0.03 mmoles C m^{-2} d^{-1}. The EA had a pCO_2 value similar to that of the CB (~514 µatms) as well as similar CO_2 flux of ~0.5 mmoles ± 0.03 C m^{-2} d^{-1}. Air-sea CO_2 flux in the WA was ~0.3 ± 0.02 mmoles C m^{-2} d^{-1}, similar to the EA and CB, but had a slightly lower pCO_2 of ~482 µatms.

Surface waters during the winter of 2012 were oversaturated in CO_2 with respect to the atmosphere and all regions experienced outgassing, while the average wind speed at this time was ~2.1 m s^{-1}. Regional pCO_2 values were more constrained, especially within the arms and the CB, ranging from ~400 µatms in the WA and CB to ~432 µatms in the EA. Similar pCO_2 values, as well as similar seawater temperatures (~3.5°C), led the WA and CB to experience similar CO_2 fluxes of ~0.03 ± 0.002 and 0.06 ± 0.003 mmoles C m^{-2} d^{-1}. The EA had a slightly higher surface temperature (~4.1°C) and flux, with ~0.18 ± 0.01 mmoles C m^{-2} d^{-1}. The LB had a slightly higher CO_2 flux of ~0.76 ± 0.04 mmoles C m^{-2} d^{-1}.

In the spring, seawater temperatures increased slightly to ~5°C across the bay while salinity remained similar to values observed during the winter (~29 to 31). However, all regions, except for the LB, transitioned to sinks for atmospheric CO_2. pCO_2 in the LB remained oversaturated with respect to CO_2 at ~423 µatms and had a flux of ~0.11 ± 0.01 mmoles C m^{-2} d^{-1}. Within the other three regions of the bay, surface water temperatures increased slightly, by just over 1°C. However, DIC and pCO_2 decreased in

the surface waters and these regions acted as sinks for atmospheric CO_2. The EA had the greatest decrease in pCO_2, dropping from ~432 µatms to ~167 µatms and exhibiting seasonal outgassing of ~ -0.87 ± 0.04 mmoles C m^{-2} d^{-1} in the spring. The CB and WA regions were also seasonal sinks for CO_2 during spring, taking up ~ -0.39 ± 0.02 mmoles C m^{-2} d^{-1} in the CB and ~ -0.60 ± 0.03 mmoles C m^{-2} d^{-1} in the WA.

During the summer of 2012 pCO_2 in the EA increased from the spring, though it was still less than atmospheric at ~337 µatms and led to ~ -0.13 ± 0.01 mmoles C m^{-2} d^{-1} of ingassing. The sink signal within the CB was larger, having a lower pCO_2 of ~200 µatms and a flux of ~ -0.44 ± 0.02 mmoles C m^{-2} d^{-1}. The remaining regions, the LB and WA, acted as sources for atmospheric CO_2 during this summer with pCO_2 values of ~411 µatms and ~507 µatms, respectively. During the summer of 2012, the LB experienced a near-neutral flux of ~0.04 ± 0.002 mmoles C m^{-2} d^{-1}. The WA was oversaturated with respect to atmospheric CO_2 with a pCO_2 of ~507 µatms and a flux of ~0.26 ± 0.01 mmoles C m^{-2} d^{-1}.

5.0 Discussion

During the summer of 2011 variability in DIC concentrations within the surface waters was a result of primary production and dilution from glacial discharge (Reisdorph and Mathis, 2014) and had the lowest concentrations in the arms due to the greater influence of glacier runoff, as well as the upper-CB, where, seasonally, chl *a* concentrations have been observed to be highest (Etherington et al., 2007). Below the surface layer, DIC and nitrate concentrations followed the Redfield ratio and were fairly constant throughout the year. Nitrate and phosphate concentrations in the surface waters were not observed to reach depletion during the summer, indicating that they were being

continuously supplied to the surface layer and that phosphate was not limiting. Sustained nutrient concentrations and nutrient replenishment may be the result of several physical interactions within the bay, including wind, tidal and internal wave mixing, especially over shallow sills at the mouth of the bay and at the entrance to the EA. Some data and literature suggests that internal waves may form within the LB in an area of station 02, known as Sitakaday Narrows. This is an area of constriction with accelerated currents that can produce hydraulic instabilities, potentially causing internal waves that may influence mixing at depth as well as at a distance from this region (Hooge & Hooge, 2002). However, additional study needs to be done to identify if, when and where in GLBA these internal waves form and to what extent they may impact mixing in that region.

Reduction in macronutrient concentrations, as well as DIC, within the more northern arms of the bay was due to primary production coupled with the influence of glacier runoff and salinity-driven stratification limiting mixing and nutrient replenishment in the mixed layer. Additionally, several glaciers in GLBA calve directly into the water rather than travel down streambeds that are rich in carbonate and organic sediments, there is little opportunity for the glacial melt to accumulate macronutrients, as is the case with carbonate alkalinity (Reisdorph and Mathis, 2014).

In the fall of 2011, DIC and nitrate concentrations increased in the surface waters as primary production slowed and wind mixing increased. Due to decreasing primary production, concentrations were similar within surface waters with the lowest concentrations observed in the arms where glacial runoff was still impacting surface waters. Increased wind mixing and the reduction of glacial input during the winter of

2012 led to deeper water column mixing, with much more constrained DIC and nitrate concentrations than during the previous seasons, with little difference (< 50 μmoles kg^{-1}) between surface and bottom waters.

Macronutrient and DIC concentrations continued to increase in the surface waters due to increased wind mixing during the winter. DIC and nitrate concentrations fell near the Redfield ratio, but deviated slightly from Redfield at the highest nitrate concentrations (Fig. 2). This may have been due to nitrification of ammonium by bacteria leading to an increase the nitrate concentration. Another possibility is 'carbon overconsumption', the process in which more DIC is taken up than that inferred from the C:N Redfield ratio (Voss et al., 2011). Explanations for carbon overconsumption include the preferential remineralization of organic nitrogen (Thomas and Schneider, 1999) or an increased release of dissolved organic carbon (DOC) (Engel, et al., 2002; Schartau et al., 2007).

As temperatures began to warm in the spring of 2012, the onset of glacial melt and primary production reduced DIC and nitrate concentrations in surface waters across the bay. During the spring DIC and nitrate correlated closely with the Redfield ratio except for two surface samples located at the northernmost ends of each arm (Fig. 2). This deviation may be explained by the fact that these stations were the first to be influenced by glacial runoff during the onset of the glacial melt season.

Further reduction in DIC and nitrate concentrations in surface waters was observed during the summer of 2012 as primary production intensified. Low nutrient glacial runoff was also highest at this time of year, affecting surface water macronutrient concentrations within the arms of the bay (Hooge & Hooge, 2002). However,

concentrations did not drop as low as was observed during the previous summer. Similar to the previous summer, macronutrients did not reach depletion during the summer of 2012, implying they were not the limiting primary productivity, possibly due to nutrient replenishment via tidal pumping. As shown in Figure 2, the surface nitrate concentration continued to deviate from the Redfield ratio as these macronutrients were increasingly drawn down by primary productivity and diluted by glacier runoff. The stations most affected were those within the EA and WA, as well as upper CB, where freshwater influence was greatest. Mixing of nutrient-rich marine waters from the GOA likely offset much of the drawdown from primary production and allowed these surface waters to fall closer to the Redfield ratio within the LB.

The seasonal transition between the summer and fall of 2011 had the largest rates of NCP observed during the year of study. During this time all NCP rates were positive, signifying enhanced primary productivity in the mixed layer. Rates of NCP became negative during the seasonal transitions from fall to winter, as well as from winter to spring. These negative NCP values indicate that air-sea fluxes (discussed in Section 4.5) and organic matter respiration were prominent, increasing CO_2 (DIC) concentrations in the surface waters and overwhelming any weaker signal from primary production. Air-sea flux of CO_2 overwhelmed the biological signal in all regions of GLBA between the fall and winter seasons. Between the fall and winter, the LB experienced the highest degree of CO_2 flux when compared to biological production. The biological production was overwhelmed by CO_2 influx in the east and west arms, but to a less degree than in regions to the south.

A similar trend was observed between the winter and spring of 2012 in all regions

except for the LB, likely due to its more macronutrient-rich marine influence from the GOA. The CO_2 flux signal exceeded NCP within the east and west arms of the bay, as well as the CB, though rates in the CB were about half that of the EA. The LB was the only region where biological production dominated the CO_2 flux with a positive NCP rate, again reflecting the region's nutrient-rich marine influence. During the transition from the spring to summer of 2012 primary production signal was evident in the NCP rates. The highest rate of NCP was estimated within the LB, while rates within the CB and EA were of similar magnitude. The WA experienced a lower rate of NCP, possibly the result of the strong low-macronutrient glacial influences along the arm, which may work to hinder production. Additionally, large volumes of glacial flour imparted into the surface waters from runoff during summer may have limited the photic depth and thus impeded some productivity in the upper arms of the bay (Etherington et al., 2007).

The total mass of carbon produced via NCP was estimated for each seasonal transition (Fig. 4). Between the summer and fall of 2011, we observed the greatest production of organic carbon of any seasonal transition, with the largest production signal in the LB and decreasing to the north as glacial influence increased. The LB had the largest production signal, possibly due to continued nutrient replenishment to surface waters as a result of interactions with the more marine waters outside of the bay. Production was also high in the CB, followed by the more glacially influence east and west arms. As with the rates of NCP during seasonal transitions with low biological activity, the strong influence of air-sea CO_2 flux can be seen in the masses of carbon calculated. Any negative carbon masses indicate a gain in carbon within the surface waters as a result of low biological production and high wind-induced CO_2 flux and

community respiration.

Transitioning from fall to winter, there was substantial contrast between the marine-dominated LB and the glacially-influenced EA. All regions were dominated by air-sea CO_2 flux during this time, indicated by negative masses of carbon production. This differences in magnitude of these estimates between the northern and southern regions was likely the result of a higher degree of wind and tidal mixing at stations outside of and near the mouth of the bay.

The production estimates within the arms and central regions of the bay continued to be overwhelmed by air-sea flux between the winter and spring of 2012. While production estimates remained negative in the northern regions of the bay, the LB once again had a positive NCP mass signifying increased primary production and a decrease in air-sea flux in this region.

Between the spring and summer there was increased production across the bay as stratification strengthen and the hours of daylight increased. The largest production was again within the LB. During this time of the year the east and west arms exhibited the lowest biomass production. NCP was likely hindered within the arms by the inundation of low-nutrient glacial runoff that formed a fresh surface layer and imparted glacial flour into the surface waters in these regions.

During the summer of 2011 surface water POC concentrations were generally elevated within the surface waters, with lower concentrations below this layer. Within the CB, POC concentrations below the surface relatively low, while the surface waters had a POC concentrations almost three times greater, indicating relatively high primary production in the surface waters, but little export to depth, perhaps due to reutilization within the surface waters or horizontal advection from tidal action. In contrast, the LB had relatively lower POC concentrations, but they were similar at all depth. This could have been the result of higher turbulent mixing within the surface waters outside of the bay leading to weaker stratification and increased vertical mixing, as well as resuspension

of POC sediment above and around the shallow entrance sill. Stations at the head of the EA had elevated POC concentration at all sampled depths. The elevated concentrations at these stations may have been due to high erosion and sedimentation of recently grounded Muir glacier. The WA exhibited the highest sub–surface POC concentrations, while surface waters in both arms also exhibited negative AOU values indicating high primary production within these regions.

Concentrations of POC fell rather dramatically, especially within the surface waters as primary production slowed during the fall. The highest POC concentration was observed in the surface waters of the WA, while surface concentrations within the other three regions were comparable. At depths below the surface, POC concentrations were low, while all AOU values were positive during the fall of 2011, indicating widespread organic matter respiration. During the fall the LB, especially across and seaward of the sill, were well mixed at this time of year (Reisdorph and Mathis, 2014) and experienced a high degree of air-sea gas exchange (see section 4.5), which likely lowered the oxygen concentration. This region had the highest DIC concentrations and lowest oxygen saturation, suggesting turbulent mixing enhanced air-sea flux, taking up DIC and outgassing oxygen.

During the winter, surface water POC concentrations remained low and AOU values were elevated, suggesting little production was occurring within the bay, but respiration was present. This is further supported by the negative NCP values described in Section 4.2. Regional POC maxima were observed in the bottom waters within the EA and LB. In the LB, where NCP was lowest, the bottom water POC concentration may have been the result of turbulent mixing outside of and across the sill of the bay, which

can mix the water column to depth in this region (Reisdorph and Mathis, 2014; Etherington et al., 2007) and likely stir up sediments along the bottom.

With the onset of primary production during the spring, POC concentration in the surface waters began to rise, primarily within northern regions of the bay. Surface POC concentrations were highest in the northern regions where the onset of the glacial melt season imparts freshwater that can help establish the stratification essential for primary production, The LB experienced the lowest surface POC concentrations, while having the highest rate of NCP. However, the LB subsurface and deep water POC concentrations were the highest of the four regions and the only region to have a positive AOU in bottom waters, suggesting a larger vertical transport of organic particles out of the surface layer than was observed in other regions.

During the summer of 2012, all four regions exhibited regionally averaged POC maxima at the surface, decreased AOU values and had elevated rates of NCP indicating substantial productivity within these waters. The EA had the highest surface concentration of POC, possibly the result of high productivity and strong stratification due to the buoyant glacial melt layer, prohibiting particles from sinking out of the surface layer. However, the LB generally experiences a higher degree of turbulent mixing over and outside of the entrance sill that can lead to higher export production in this region. Low surface POC concentration in the LB, coupled with a high rate of NCP during this season was likely the result of more rapid sinking rates of particles out of the surface waters in these more turbulent waters than in the more glacially-stratified northern regions of the bay.

DIC and DO are both indicators of biological production in a marine ecosystem

and have a C:O Redfield ratio of 106:-170 (Anderson et al., 1994). DIC and DO have an inverse relationship in that DIC is taken up during photosynthesis, while DO is produced, so we would expect high oxygen saturation states in spring and summer months. During the summer of 2011, all samples below the surface layer, as well as surface samples within the LB followed the Redfield ratio relatively well (Fig. 6). Surface samples within the CB and arms deviated from Redfield, with elevated DO concentrations and reduced DIC than would be expected via biological processes alone. These waters were influenced by low macronutrient glacial runoff that diluted these concentrations and, coupled with primary production, further reduced these concentrations in the surface waters. The high DO concentrations, coupled with the reduced DIC concentrations in the surface waters indicate enhanced levels of primary production during the summer season.

During fall DO concentrations decreased in the surface waters as temperatures cooled and wind mixing reduced stratification, hindering primary production within the surface waters. However, the surface samples within the arms and CB continued to deviate from Redfield. Surface DO concentrations were coupled with reduced surface DIC concentrations suggesting primary production was still occurring, albeit at a lesser level than summer.

The water column throughout the bay was well mixed during the winter of 2012. During this time of year primary production is low and turbulent mixing is at a peak. All samples, at the surface and at depth, clustered along the Redfield line (Fig. 6) with surface samples exhibiting slightly higher DO concentrations than waters at depth, perhaps due to a higher degree of respiration in these waters following summer and fall primary production.

As stratification increased during the spring, production in the surface waters increased, drawing down DIC and increasing DO concentrations in surface waters. This was most notable in the northern-most regions of the arms where samples deviated the most from Redfield. This may have been a result of an earlier onset of stratification as a result of the fresh glacial runoff into these regions, enhancing stratification as compared to the more marine southern regions of the bay.

Surface water DIC and DO concentrations within the arms and CB continued to diverge from Redfield during the summer of 2012. DIC concentrations within the EA, WA, and CB continued to decrease, while DO concentrations remained high, indicating strengthening productivity in the surface waters.

While GLBA itself represents only a small portion of Alaska's coastal environment, the coastal ocean surrounding the GOA has been shown to act as an important sink for atmospheric CO_2 when averaged seasonally, with uptake of 2.5 to 4 mmoles C m^{-2} d^{-1} (Evans and Mathis, 2013). In GLBA, air–sea fluxes varied regionally and seasonally between the summer of 2011 and the summer of 2012.

In the summer of 2011 regions of oversaturation and undersaturation with respect to the atmospheric CO_2 were observed. At this time winds were relatively low, reducing turbulent mixing, allowing for stratification and, thus, primary production. Surface waters of the CB and the WA acted as sinks for atmospheric during this season, while the LB and EA were sources. The CB has been observed to have abundant chl. *a* levels during most of the year (Hooge & Hooge, 2002) suggesting enhanced primary production that would act to decrease DIC concentrations and pCO_2 in this region. The WA also had reduced DIC concentrations during this summer largely due to the influx of low-

macronutrient tidewater runoff. As a result, lower DIC values caused the CB and the WA to act as minor sinks. The LB and EA had seawater pCO_2 values greater than those of the atmosphere causing these regions to act as a source for atmospheric CO_2. Within the lower and central regions of the bay surface water temperatures were relatively high. Additionally, the LB experiences turbulent mixing due to tidal action across the shallow sill, which can act to inhibit strong stratification and enhance air-sea gas exchange. Within the EA it was likely the influence of low-TA glacial runoff that led to this region's source status. This runoff, low in TA, increased the pCO_2 in the surface waters. During this time of year seawater temperatures were also rising, increasing the pCO_2 of these waters. The combined influence of the reduced TA concentrations and increased temperatures resulted in an oversaturation of CO_2 in the seawater with respect to the atmosphere and overwhelmed any effect from DIC drawdown via primary production.

Transitioning to the fall of 2011, winds increased slightly and all surface waters across the bay experienced oversaturation with respect to the atmospheric CO_2. The LB acted as the strongest regional source, with each of the others regions outgassing roughly half the magnitude as the LB. The high pCO_2 values observed during fall, despite strong DIC drawdown during summer, may be the result of a variety of interactions. As a result of reduced glacial runoff during fall, TA concentrations increased (Reisdorph and Mathis, 2014). Additionally, surface water temperatures declined allowing them to hold more CO_2 while mixing brought DIC-rich waters from depth to the surface. These processes likely allowed more CO_2 retention in the water, thus increasing pCO_2 and making the bay a source for CO_2 to the atmosphere.

During the winter of 2012 surface waters across all regions of the bay continued to be oversaturated with respect to atmospheric CO_2 and experienced outgassing. However, fluxes were much lower than during the fall. Once again the LB experienced the largest degree of outgassing, like due to its more turbulent mixing, especially across and seaward of the entrance sill. Despite winter having the lowest seawater temperatures, wind mixing peaked and allowed for CO_2-rich waters from depth to enter the surface waters, increasing pCO_2.

Several regions of GLBA transitioned to sinks for atmospheric CO_2 during the spring of 2012. The LB was the exception, remaining oversaturated with respect to CO_2 and continuing to act as a minor source for atmospheric CO_2, likely the result of greater turbulent flow seaward of the sill delaying the formation of strong stratification and inhibiting primary production. In the more northern regions, surface water experienced a slight increase in surface temperatures, but due to the onset of spring productivity DIC was drawn down in the surface waters, decreasing the pCO_2 and allowing them to become sinks for atmospheric CO_2. The EA experienced that large decrease in pCO_2, allowing it to become the largest sink region within the bay during the spring, while the WA and CB underwent similar transitions, becoming sinks for atmospheric CO_2. The reduction in pCO_2 within these regions was the result of increased primary production drawing down DIC in the surface waters causing them to become a seasonal sink for CO_2.

Over- and undersaturation of CO_2 in surface waters varied regionally, with waters in the northern regions becoming increasingly saturated with respect to atmospheric CO_2. While, pCO_2 in the EA did increase from spring values, it was still undersaturated with

respect to atmospheric pCO_2, leading to ingassing in this region. The increase in pCO_2 may have been due to a small increase in seawater temperature, coupled with a reduction in TA (Reisdorph and Mathis, 2014) overwhelming the drawdown in DIC from primary production. Uptake within the CB strengthened slightly from the as pCO_2 in this region decreased. This reduction in pCO_2 was likely due to high levels of primary production in this region as it has been noted to have some of the highest chl. *a* levels, as well as high nutrient replenishment from tidal mixing between the mixed waters of LB and the stratified waters within the CB (Hooge & Hooge, 2002). Conversely, the LB remained a minimal source for atmospheric CO_2, while the WA transitioned into source during the summer. The LB experiences the highest degree of turbulent or tidal mixing across the sill, as well as seaward of the sill, inhibiting stratification and primary production and causing it act as a source for atmospheric CO_2 year-round. The difference in the sink/source status of the east and west arms of the bay was likely the result of differences in glacial influences. The WA is much more influenced by low-TA glacial runoff as it has the majority of the tidewater glaciers along its length. During the summer of 2012, these glaciers caused a higher degree of TA dilution than was observed within the WA. The upper end of WA also had the lowest DIC concentrations observed during this summer also likely due to the high tidewater glacier runoff, which tends to be lower in macronutrients.

6.0 Conclusions

GLBA experiences a high degree of spatial and temporal variability in biogeochemical characteristics throughout the year. Environmental influences vary

seasonally along a gradient from the glacially-influenced northern regions within the arms to the marine-influenced LB. This imparts spatial differences in stratification and macronutrient availability that effect biological processes and thus, rates of NCP.

We have calculated regional NCP values for each seasonal transition from the summer of 2011 through summer 2012 for GLBA. Despite GLBA's limited exchange with the marine waters of the GOA, it has been observed to support elevated primary production through most of the year (Hooge & Hooge, 2002), perhaps due to tidal pumping, and has a marine predator presence in all season. However, rapid deglaciation within GLBA over the past ~250 years has imparted a high volume of fresh glacial runoff, a portion of which has been from tidewater glaciers that melt directly into the bay, affecting stratification, macronutrient concentrations and influencing air-sea CO_2 exchange.

Between the summers of 2011 and 2012, nutrient concentrations in GLBA tended to be lowest in the surface waters of the arms, though never reaching depletion, during the summer season when glacial runoff, primary production (Fig. 2), and DO concentrations (Fig. 6) were highest. Rates of NCP were highest during the transition between summer and fall of 2011, with regional NCP rates ranging from ~54 to ~80 mmoles C m^{-2} d^{-1}. Rates during the summer of 2012 were lower, between ~6 and ~20 mmoles C m^{-2} d^{-1}.

Between the fall of 2011 and winter of 2012, as well as between the winter and spring of 2012, air-sea gas exchange overwhelmed any production signal across the bay. The one exception was LB between winter and spring where NCP rates were positive, likely due to earlier replenishment of nutrients from marine source waters. Although air-

sea flux overwhelmed NCP seasonally, fluxes were minimal, with maximum outgassing of ~1.1 mmoles C m^{-2} d^{-1} occurring in LB during the fall of 2011. While the direction of fluxes varied seasonally and regionally, LB acted as a small source for atmospheric CO_2 during all seasons of the study. During the summer of 2012 areas of CO_2 over- and undersaturation varied, with the LB and WA acting as sources for atmospheric CO_2 and the CB and EA acting as sinks. NCP followed this pattern with a maximum in the LB of $8.0x10^9$ g C $season^{-1}$, followed by the CB with $8.5x10^8$ g C $season^{-1}$. NCP was lowest within the WA ($9.2x10^7$ g C $season^{-1}$), likely due to low-TA, low-macronutrient tidewater glacier runoff slowing primary production. Despite a sustained level of primary production in the WA, pCO_2 in this region remained oversaturated (~506 μatm) with respect to the atmosphere. This was attributed to the low-TA glacial runoff diluting TA concentrations in the surface water leading to elevated pCO_2. This, coupled with the fact that these warmer summer waters have inherently higher pCO_2, caused pCO_2 levels to remain elevated despite sustained biological production. It is clear from our observations that highly glaciated systems like GLBA behave much differently than open ocean regions, as well as glaciated systems with less restricted marine exchange like PWS, when it comes to CO_2 fluxes. The complex interactions between NCP, temperature and TA cause GLBA to behave much differently than the adjacent GOA, which has been shown to be a significant sink for atmospheric CO_2 (Evans and Mathis 2014).

The impact of rapid deglaciation in GLBA can be observed in the seasonal impacts on the biogeochemistry of this marine system. This study adds to the understanding of the impacts of glacial melt on estuarine biogeochemistry, as well as the limited biogeochemical literature regarding GLBA. It includes one of the more robust

datasets from GLBA, while also enhancing the study of glacially–influenced estuaries along the Alaskan coast that, together, can play a large role in global carbon fluxes. The influence of surrounding glaciers, especially tidewater glaciers, has the potential to significantly impact the efficiency and makeup of the marine food web within GLBA. Some prey species, such as capelin, thrive nearest the tidewater glaciers, most of which are currently receding and thinning, leaving these species with a smaller, less optimal habitat and affecting predators within higher tropic levels. A similar occurrence in the GOA saw a decline in predator species, such as harbor seals and red-legged kittiwakes, as the result of glacial recession (Aritmisu, 2008). The full impact that deglaciation has on a marine system like GLBA, and the numerous similar systems along the Alaskan GOA coast, is currently unknown. However, the coastal margin of the GOA has been estimated at ~3000 km, or ~1.5 times the length of the U.S. continental margin between northern Washington and southern California and, therefore needs more study and should be considered an area of vital importance to the regional carbon budget.

Acknowledgments

Thanks to the National Park Service for supporting this work through grant number G7224 to the University of Alaska Fairbanks. We would also like to thank Lewis Sharman and NPS staff members in Gustavus and Juneau, AK for their help in sample collection, logistics and editing. We also want to thank the staff and visitors of Glacier Bay National Park and Preserve, as well as the community of Gustavus for their support and interest in this project.

References

Anderson, L.A., Sarmiento, J.L., 1994. Redfield ratios of remineralization determined by nutrient data analysis. Global Biogeochem. Cycles 8, 65–80.

Aracena, C., Lange, C.B., Luis Iriarte, J., Rebolledo, L., Pantoja, S., 2011. Latitudinal patterns of export production recorded in surface sediments of the Chilean Patagonian fjords (41–55°S) as a response to water column productivity. Cont. Shelf Res. 31, 340–355. doi:10.1016/j.csr.2010.08.008

Arimitsu, M.L., Piatt, J.F., Litzow, M. A., Abookire, A. A., Romano, M.D., Robards, M.D., 2008. Distribution and spawning dynamics of capelin (*Mallotus villosus*) in Glacier Bay, Alaska: a cold water refugium. Fish. Oceanogr. 17, 137–146. doi:10.1111/j.1365-2419.2008.00470

Bates, N.R., Best, M.H.P., Hansell, D. A., 2005. Spatio-temporal distribution of dissolved inorganic carbon and net community production in the Chukchi and Beaufort Seas. Deep Sea Res. Part II Top. Stud. Oceanogr. 52, 3303–3323. doi:10.1016/j.dsr2.2005.10.005

Cross, J.N., Mathis, J.T., Bates, N.R., 2012. Hydrographic controls on net community production and total organic carbon distributions in the eastern Bering Sea. Deep Sea Res. Part II Top. Stud. Oceanogr. 65-70, 98–109. doi:10.1016/j.dsr2.2012.02.003

Engel, A., Goldthwait, S., Passow, U., Alldredge, A., 2002. Temporal decoupling of carbon and nitrogen dynamics in a mesocosm diatom bloom. Limnol. Oceanogr. 47, 753–761. doi:10.4319/lo.2002.47.3.0753

Etherington, L., Hooge, P.N., Hooge, E.R., Hill, D.F., 2007. Oceanography of Glacier Bay, Alaska: implications for biological patterns in a glacial fjord estuary. Estuaries and Coasts 30, 927–944.

Evans, W., Mathis, J.T., 2013. The Gulf of Alaska coastal ocean as an atmospheric CO2 sink. Cont. Shelf Res. 65, 52–63. doi:10.1016/j.csr.2013.06.013

Gelatt, T.S., Trites, A.W., Hastings, K., Jemison, L., Pitcher, K., and O'Corry-Crow, G., 2007, Population trends, diet, genetics, and observations of steller sea lions in Glacier Bay National Park, *in* Piatt, J.F., and Gende, S.M., eds., Proceedings of the Fourth Glacier Bay Science Symposium, October 26–28, 2004: U.S. Geological Survey Scientific Investigations Report 2007-5047, p. 145-149.

Goñi, M. A., Teixeira, M.J., Perkey, D.W., 2003. Sources and distribution of organic matter in a river-dominated estuary (Winyah Bay, SC, USA). Estuar. Coast. Shelf Sci. 57, 1023–1048. doi:10.1016/S0272-7714(03)00008-8

Helmuth, T., Schneider, B., 1999. The seasonal cycle of carbon dioxide in Baltic Sea surface waters. J. Mar. Syst. 22, 53–67.

Hill S.J. Ciavola, L. Etherington, M.J. Klaar, D.F., 2009. Estimation of freshwater runoff into Glacier Bay, Alaska and incorporation into a tidal circulation model. Estuar. Coast. Shelf Sci. 82, 95–107.

Hooge, E. R., Hooge, P.N., 2002. Fjord oceanographic processes in Glacier Bay, Alaska, Glacier Bay Report. Gustavus, AK.

Hooge, P.N., Hooge, E.R., Solomon, E.K., Dezan, C.L., Dick, C.A., Mondragon, J., Reiden, H.S., Etherington, L.L., 2003. Fjord oceanography monitoring handbook: Glacier Bay, Alaska. U.S Geol. Surv.1-75.

Langdon, C., 2010. Determination of dissolved oxygen in seawater by Winkler titration using the amperometric technique. GO-SHIP Repeat Hydrogr. Manual: A Collection of Expert Reports & Guidelines. 14, 1–18.

Lee, K., 2001. Global net community production estimated from the annual cycle of surface water total dissolved inorganic carbon. Limnol. Oceanogr. 46, 1287–1297. doi:10.4319/lo.2001.46.6.1287

Mathis, J.T., Bates, N.R., Hansell, D. A., Babila, T., 2009. Net community production in the northeastern Chukchi Sea. Deep Sea Res. Part II Top. Stud. Oceanogr. 56, 1213–1222. doi:10.1016/j.dsr2.2008.10.017

Mathis, J.T. and Questel, J.M., (2013). The impacts of primary production and respiration on the marine carbonate system in the Western Arctic: implications for CO_2 fluxes and ocean acidification. Cont. Shelf Res. 67, 42-51. doi: 10.1016/j.csr.2013.04.041

Mordy, C.W., Eisner, L.B., Proctor, P., Stabeno, P., Devol, A.H., Shull, D.H., Napp, J.M., Whitledge, T., 2010. Temporary uncoupling of the marine nitrogen cycle: accumulation of nitrite on the Bering Sea shelf. Mar. Chem. 121, 157–166. doi:10.1016/j.marchem.2010.04.004

Piatt, J.F., Anderson, P., 1996. Response of common murres to the Exxon Valdez oil spill and long-term changes in the Gulf of Alaska marine ecosystem. Am. Fish. Soc. Symp. 18, 720–737.

Reisdorph, S.C., Mathis, J.T., 2014. The dynamic controls on carbonate mineral saturation states and ocean acidification in a glacially dominated estuary. Estuar. Coast. Shelf Sci. 144, 8–18.

Renner, M., Arimitsu, M.L., Piatt, J.F., 2012. Structure of marine predator and prey communities along environmental gradients in a glaciated fjord. Can. J. Fish. Aquat. Sci. 69, 2029–2045. doi:10.1139/f2012-117

Robards, M., Drew, G., Piatt, J., Anson, J.M., Abookire, A., Bodkin, J., Hooge, P., Speckman, S., 2003. Ecology of elected arine ommunities in Glacier Bay : ooplankton , orage ish , eabirds and arine ammals. Anchorage, AK; Gustavus, AK., 1-156.

Schartau, M., Engel, A., Schroter, J., Thoms, S., Volker, C., Wolf-Gladrow, D., 2007. Modelling carbon overconsumption and the formation of extracellular particulate organic carbon. Biogeosciences Discuss. 4, 13–67.

Schlitzer, R., 2013. Ocean Data View, http://odv.awi.de.

Syvitski, J. P. M., Burrell, D. C., Skei, J. M., 1987. Fjords: processes and products. Springer-Verlag Inc, New York.

Trites, A.W., Donnelly, C.P., 2003. The decline of Steller sea lions *Eumetopias jubatus* in Alaska : Mamm. Rev. 33, 3–28.

Voss, M., Baker, A., Bange, H.W., Conley, D., Cornell, S., Deutsch, B., Engel, A., Ganeshram, R., Garnier, J., Heiskanen, A.S., Jickells, T., Lancelot, C., Mcquatters-Gollop, A., Middelburg, J., Schiedek, D., Slomp, C.P., Conley, D.P., 2011. Nitrogen processes in coastal and marine ecosystems, in: Sutton, M.A., Howard, C.M., Erisman, J.W., Billen, G., Bleeker, A., Grennfelt, P., van Grinsven, H., Grizzetti, B. (Eds.), The European Nitrogen Assessment. Cambridge University Press, New York, pp. 147–176.

Wanninkhof, R., McGillis, W.R., 1999. A cubic relationship between air-sea CO_2 exchange and wind speed. Geoph 26, 1889–1892.

Weber, T.S., Deutsch, C., 2010. Ocean nutrient ratios governed by plankton biogeography. Nature 467, 550–4. doi:10.1038/nature09403

Williams, P.J., 1993. On the definition of plankton production terms: edited by: Li, W.K.W. and Maestrini, S.Y., Measurements of primary production from the molecular to the global scale. ICES Mar. Sci. Symp. 197, 9-19.

Whitney, F.A., 2011. Nutrient variability in the mixed layer of the subarctic Pacific Ocean, 1987–2010. J. Oceanogr. 67, 481–492. doi:10.1007/s10872-011-0051-2

Figures and Captions

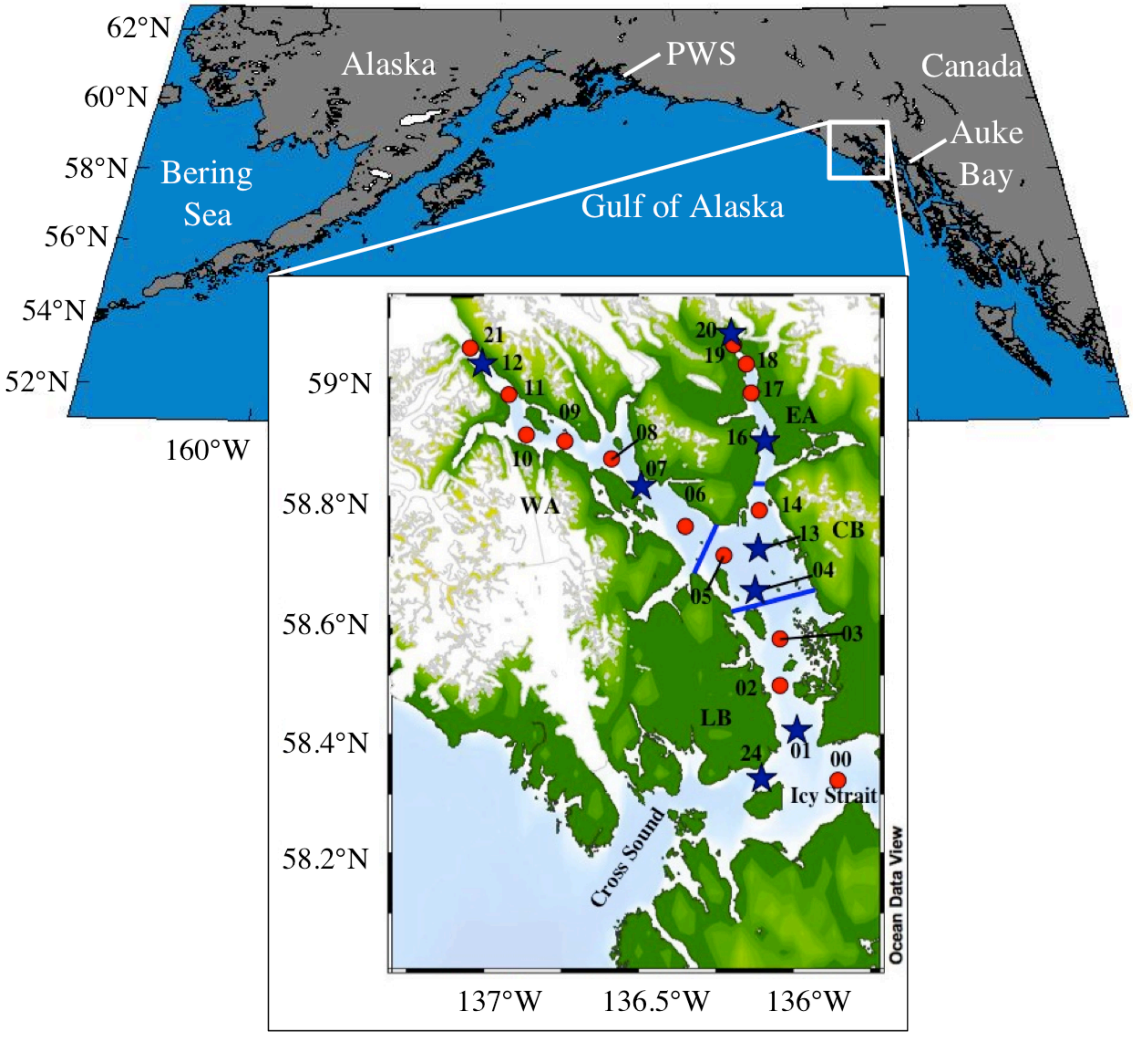

Figure 1: Glacier Bay location and oceanographic sampling station map - Blue lines denote regional boundaries. Red dots show all oceanographic station locations with station number. Purple stars represent 'core' station location. LB = lower bay, CB = central bay, EA = east arm, WA = west arm.

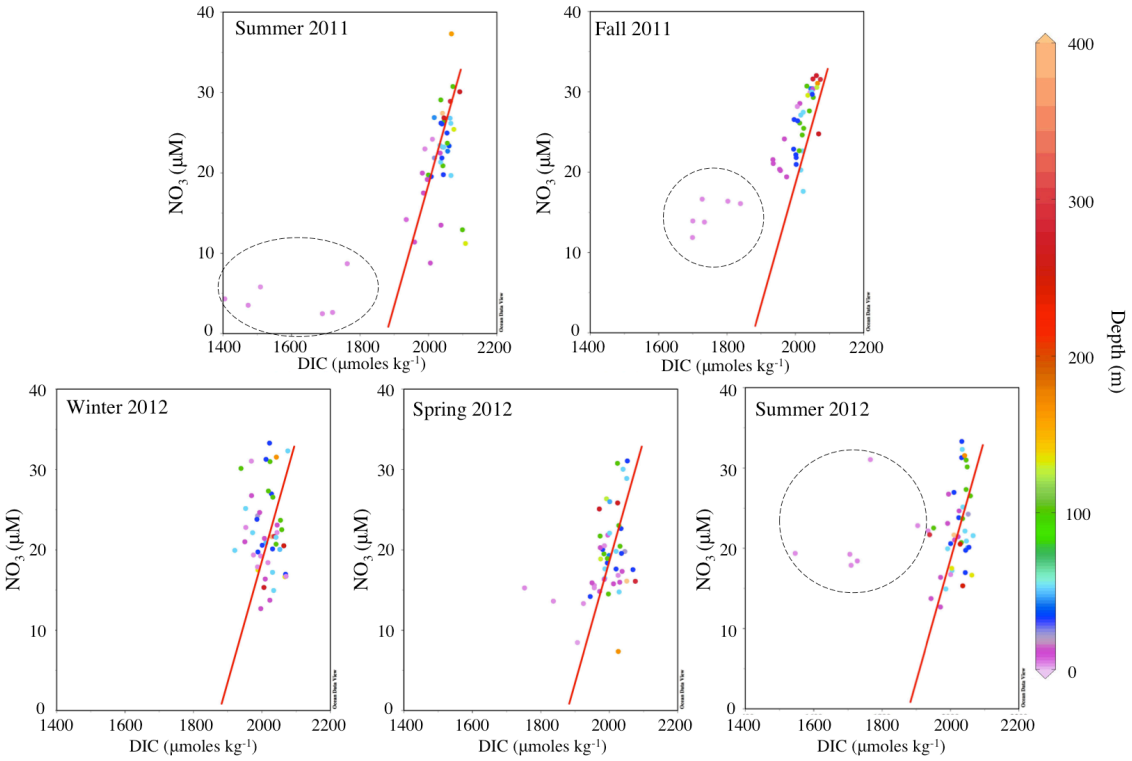

Figure 2: Seasonal DIC vs. NO_3 vs. depth - Scatter plots of DIC concentrations vs. NO_3 concentrations for each season between the summer of 2011 and the summer of 2012. Color bar represents depth in m. The red line depicts the C:N Redfield ratio of 106:16. Dotted circles highlight samples that deviate from Redfield.

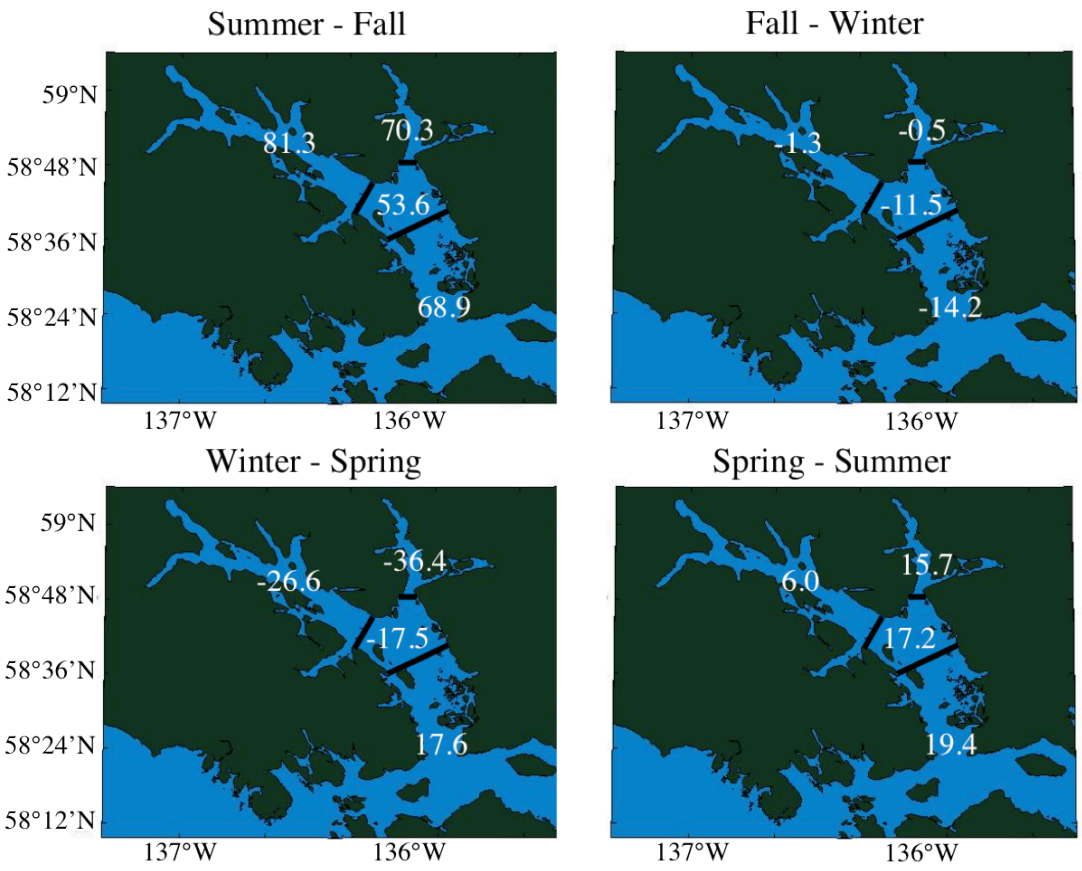

Figure 3: Regional rates of NCP - Regional rates of NCP in mmoles C m^{-2} d^{-1} for seasonal transitions from summer to fall of 2011 in the upper left through the spring to summer of 2012 in the lower right.

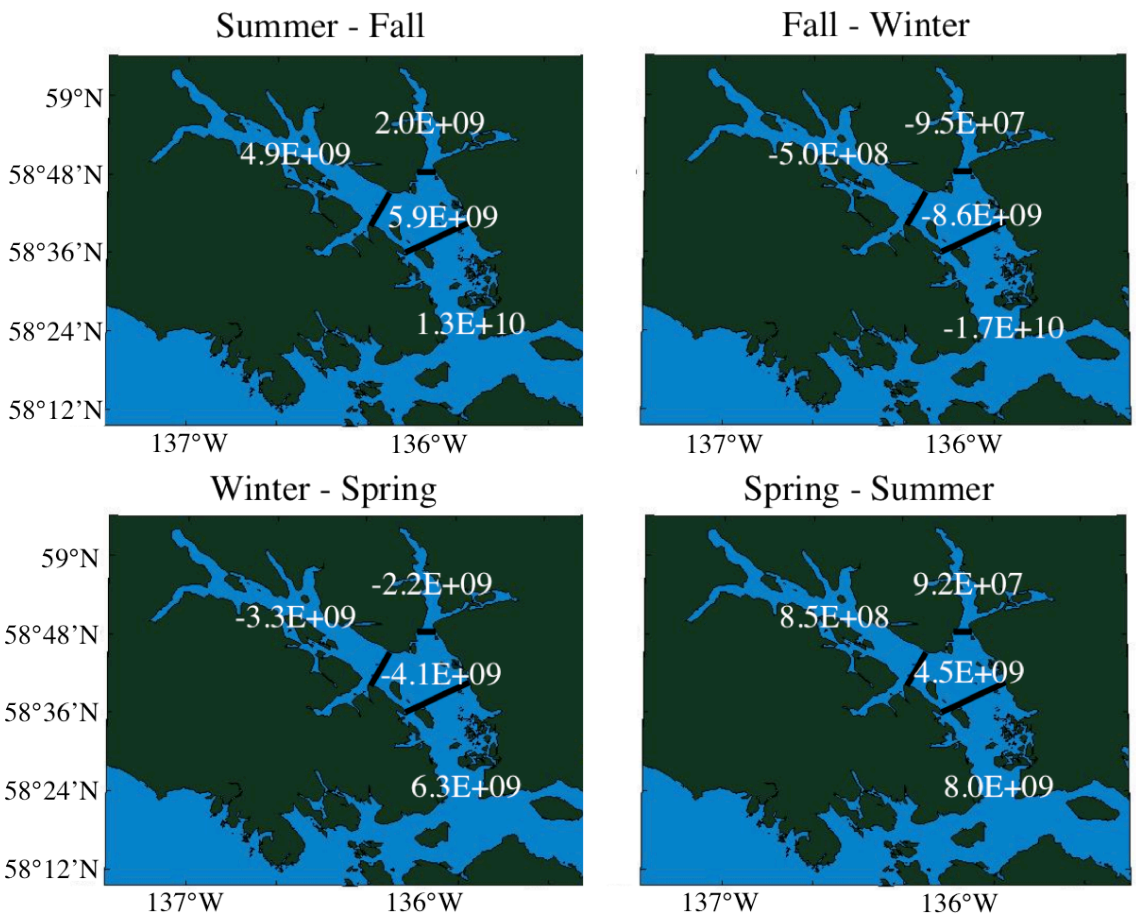

1

2 Figure 4: Regional masses of NCP - Regional masses of NCP in g C season^{-1} for seasonal

3 transitions from summer to fall of 2011 in the upper left through the spring to summer of

4 2012 in the lower right.

5

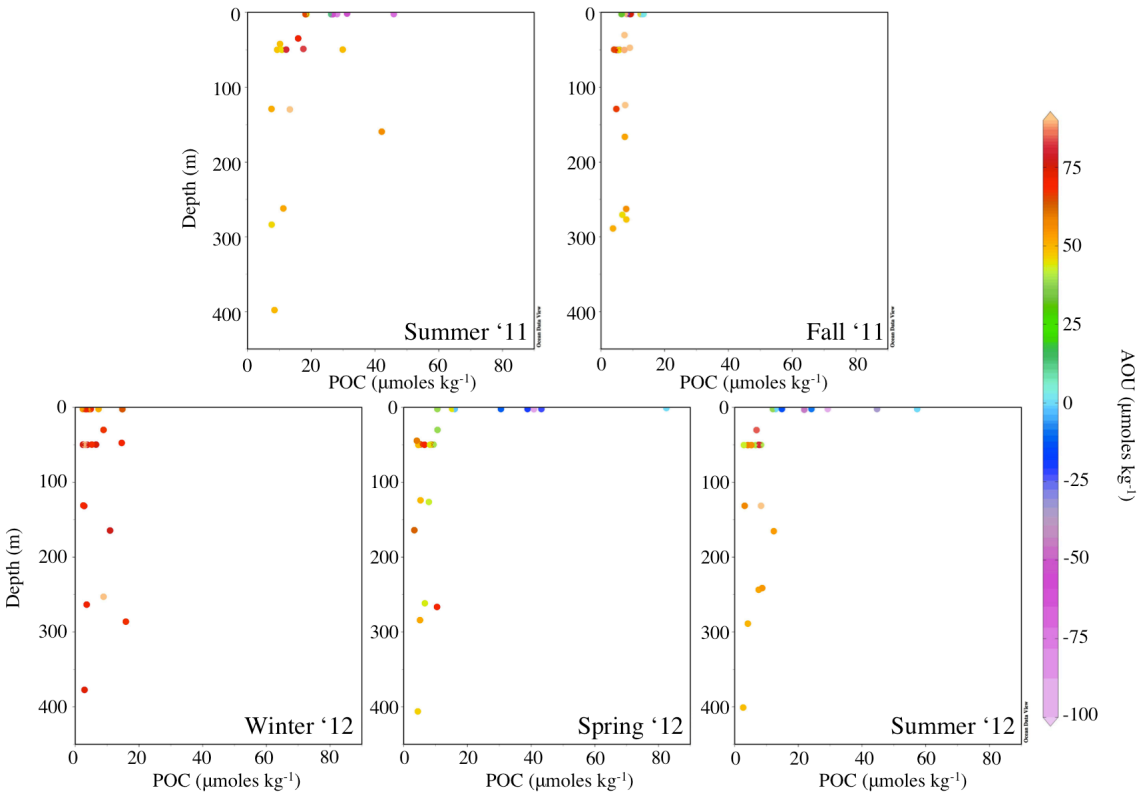

Figure 5: Seasonal POC vs. depth vs. AOU - Seasonal scatter plots of POC concentrations vs. depth for each season between the summer of 2011 through the summer of 2012. Color bar represents AOU in µmoles kg^{-1}.

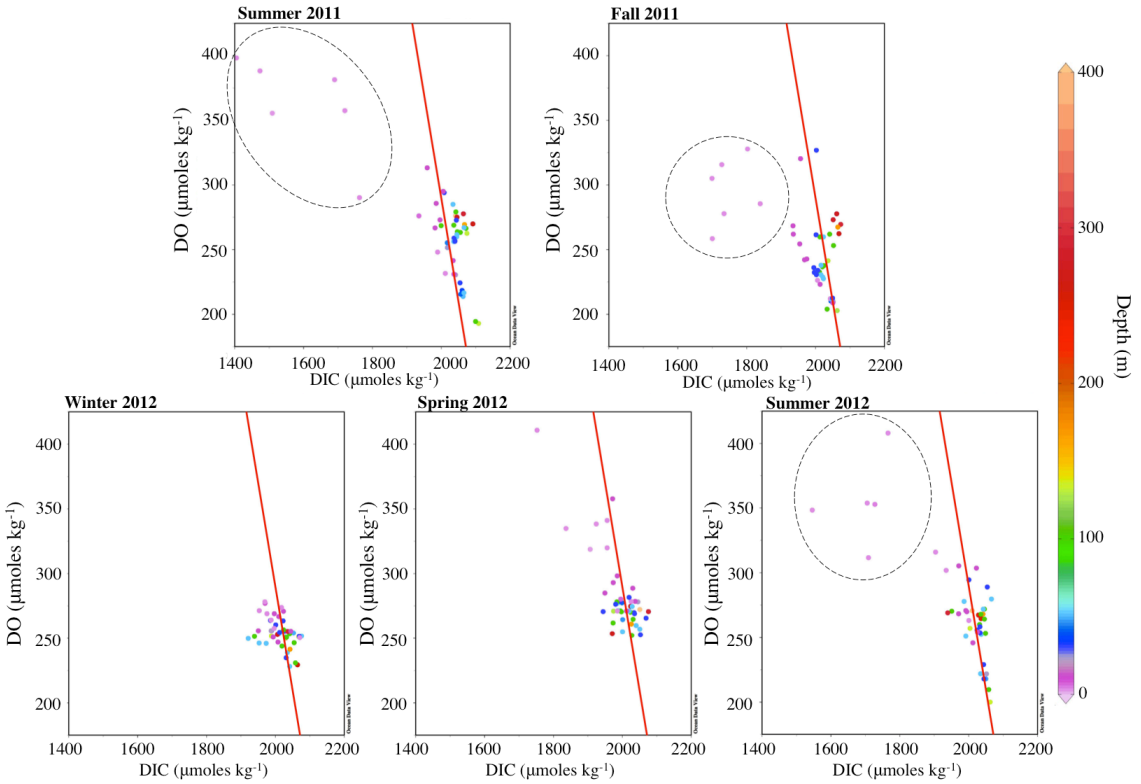

Figure 6: Seasonal DIC vs. DO vs. depth - Scatter plots of DIC concentrations vs. DO concentrations for each season between the summer of 2011 and the summer of 2012. Color bar represents depth in m. The red line depicts the C:O Redfield ratio of 106: -170. Dotted circles highlight samples that deviate from Redfield.

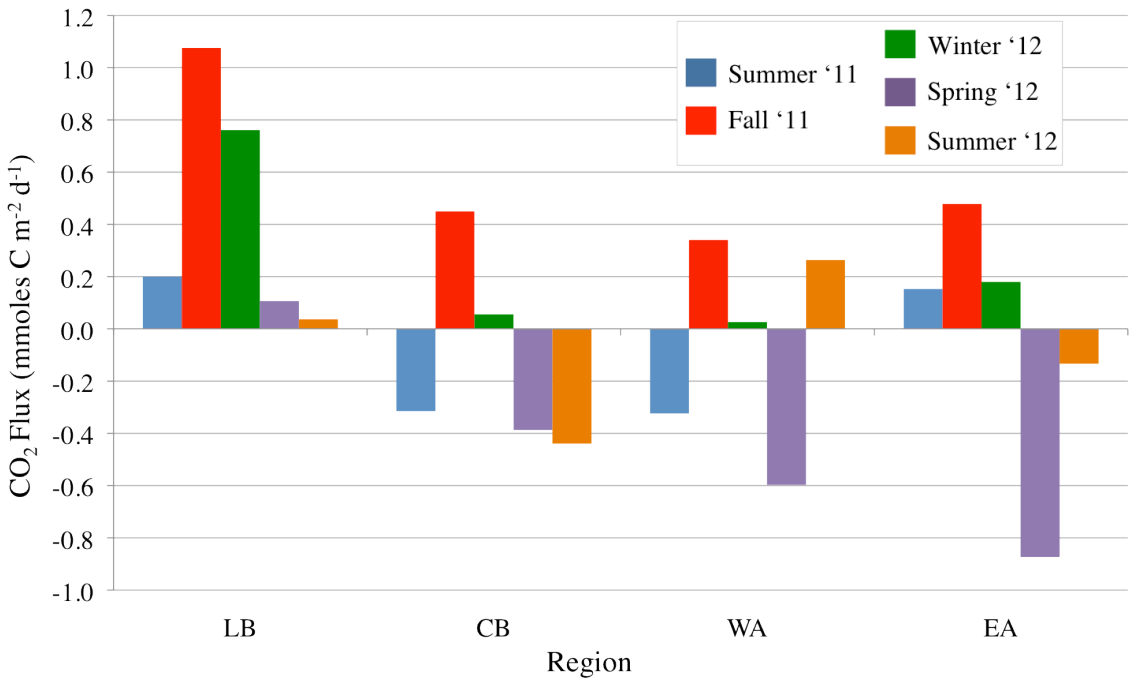

Figure 7: Air-sea CO_2 flux – Seasonal air-sea CO_2 fluxes by region in mmoles C m^{-2} d^{-1}. Blue represents the summer of 2011, red = fall of 2011, green = winter of 2012, purple = spring of 2012, yellow = summer of 2012.